5,5-Diethylbarbiturate Complexes of Silver with 2,2'-Bipyridine and 3-(2-Pyridyl)propanol: Syntheses, Crystal Structures, Spectroscopic, Thermal and Antimicrobial Activity Studies

Fatih Yilmaz[a], Veysel T. Yilmaz[b], Haydar Karakaya[c], and Orhan Büyükgüngör[d]

[a] Department of Chemistry, Faculty of Arts and Sciences, Rize University, Rize, Turkey
[b] Department of Chemistry, Faculty of Arts and Sciences, Uludag University, 16059 Gorukle, Bursa, Turkey
[c] Department of Biology, Faculty of Arts and Sciences, Ondokuz Mayis University, 55139 Kurupelit, Samsun, Turkey
[d] Department of Physics, Faculty of Arts and Sciences, Ondokuz Mayis University, 55139 Kurupelit, Samsun, Turkey

Reprint requests to Prof. Dr. V. T. Yilmaz. E-mail: vtyilmaz@uludag.edu.tr

Z. Naturforsch. **2008**, *63b,* 134 – 138; received August 28, 2007

Two silver 5,5-diethylbarbiturate (barb) complexes with 2,2′-bipyridine (bpy) and 3-(2-pyridyl) propanol (pypr), [Ag(barb)(bpy)] (**1**) and [Ag(barb)(pypr)] (**2**), have been prepared and characterized by elemental analysis, IR spectroscopy, thermal analysis, and single crystal X-ray diffraction. Both complexes crystallize in the triclinic space group $P\bar{1}$ with $Z = 2$. The barb ligand in **1** is N-coordinated and the bpy ligand acts as a bichelating ligand leading to an AgN_3 tricoordination. Crystals of **1** feature a three-dimensional network based on N–H···O hydrogen bonding, π(bpy)···π(bpy), C–H···π(bpy) and π(bpy)–Ag interactions. In **2**, the pypr and barb ligands behave as monodentate ligands through their N atoms, forming a distorted linear AgN_2 coordination. Molecules of **2** are doubly bridged by N–H···O hydrogen bonds and further connected *via* O–H···O hydrogen bonds and aromatic π(pypr)···π(pypr) stacking interactions into a supramolecular network. Both complexes exhibit similar thermal decomposition behavior in air. The first stage corresponds to removal of the co-ligands such as bpy or pypr while the degradation of the barb moiety occurs at higher temperatures to give Ag_2O. Like the barb, bpy and pypr ligands, **2** does not show any significant antimicrobial activity, but **1** is active against bacteria and fungi.

Key words: 5,5-Diethylbarbiturate, 2,2′-Dipyridine, 3-(2-Pyridyl)propanol, Silver(I), Crystal Structure

Introduction

Barbituric acid (barbH) itself is not pharmacologically active, but its derivatives produce a wide spectrum of central nervous system depression effects, from mild sedation to coma, and have been used as sedatives, hypnotics, anesthetics, and anticonvulsants [1]. However, they are highly dangerous because of the small difference between a normal dose and an overdose. Barbiturates effectively slow down the central nervous system, and with a small dose people feel relaxed, sociable and good humored, but with larger doses hostility, anxiety, loss of co-ordination and difficulty in staying awake are common effects. Barbiturates were first introduced for medical use in the early 1900s. Owing to their popularity, more than 2500 barbiturates have been synthesized, and about 50 of them have been marketed.

The presence of several potential donor sites such as two amine nitrogen and three carbonyl oxygen atoms makes barbiturates polyfunctional ligands in coordination chemistry. Levi and Hubley investigated the reaction of copper(II) with various barbiturates in the presence of pyridine (py), and on the basis of IR spectral data they suggested that the barbiturate ligands are coordinated to copper(II) *via* the carbonyl O atom [2]. However, single crystal structure analyses of the 5,5-diethylbarbiturate (barb) complexes $[Cu(barb)_2(py)_2]$ [3] and $[Zn(barb)_2(pic)_2]$ (pic = picoline) [4] confirmed that the donor atom in the barb anion is the deprotonated N atom.

Recently, we have started a project on the synthesis and characterization of the metal complexes of barb and reported a number of new complexes with various co-ligands [5 – 8]. The barb ligand in these complexes acts as an N-coordinated monodentate or bidentate lig-

0932–0776 / 08 / 0200–0134 $ 06.00 © 2008 Verlag der Zeitschrift für Naturforschung, Tübingen · http://znaturforsch.com

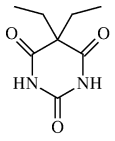

barbH

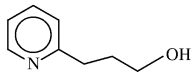

pypr

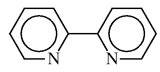

bpy

and *via* the negatively charged imino N atom and one of the carbonyl O atoms adjacent to the imino N atom. In this paper, we report the syntheses, structures, thermal behavior, and antimicrobial activities of two new silver-barb complexes with 2,2′-bipyridine (bpy) and 3-(2-pyridyl)propanol (pypr), namely [Ag(barb)(bpy)] (**1**) and [Ag(barb)(pypr)] (**2**).

Results and Discussion

Synthesis and characterization

Complexes **1** and **2** were obtained in high yields as colorless crystals by the reaction of Na(barb) with $AgNO_3$ in aqueous solution in the presence of bpy or pypr at r. t. The analytical data (C, H, and N) are consistent with the formulation of these complexes, which are non-hygroscopic and stable in air at r. t. Both complexes are highly soluble in DMF, DMSO and mixtures of water and 2-propanol, and slightly soluble in water, methanol, ethanol, and 2-propanol.

The IR spectra of complexes **1** and **2** display characteristic bands of all ligands. The strong absorption bands between 3180 and 3200 cm^{-1} correspond to the ν(NH) vibrations of the barb ligands, while the strong and broad band centered at 3362 cm^{-1} is assigned to the ν(O–H) vibration of the hydroxyl group of pypr in **2**. The medium and weak bands in the range 3100 – 2800 cm^{-1} are characteristic of both aromatic and aliphatic ν(CH) vibrations. The carbonyl group vibrations are observed as two very strong absorption bands at 1695 and 1668 cm^{-1} in **1**, and at 1660 and 1615 cm^{-1} in **2**, due to participation of the carbonyl groups in both coordination and hydrogen bonding.

The ^{1}H NMR spectra of complexes **1** and **2** exhibit signals at 10.66 and 10.69 ppm, respectively, assigned to the NH proton of the barb ion. In the NMR spectrum of **2**, the signal at 4.55 ppm corresponds to the OH group of the pypr ligand. All the other protons are also found in the spectra of both complexes.

Description of the crystal structures

The molecular structures of **1** and **2** are shown in Figs. 1 and 2, respectively. Selected bond lengths and angles are listed in Table 1 together with the hydrogen bonding geometry.

Table 1. Selected bond lengths (Å) and angles (deg), and hydrogen bonding geometry of complexes **1** and **2**[a].

1	Ag1–N1	2.3440(12)	N1–Ag1–N2	71.54(4)
	Ag1–N2	2.2523(12)	N1–Ag1– N3	130.41(5)
	Ag1–N3	2.1175(12)	N2–Ag1– N3	157.99(5)
2	Ag1–N1	2.1173(14)	N1–Ag1–N3	168.02(5)
	Ag1–N3	2.1434(15)		

Hydrogen bonds

	D–H···A	D–H	H···A	D···A	D–H···A
1	N4–H4a···O1[i]	0.86	2.00	2.8532(17)	174
2	N2–H2···O1[ii]	0.86	1.98	2.835(2)	176
	O4–H4···O3[iii]	0.82	2.04	2.821(2)	159

[a] Symmetry operations: [i] $1-x, 1-y, -z$; [ii] $2-x, 1-y, 2-z$; [iii] $x+1, y, z$.

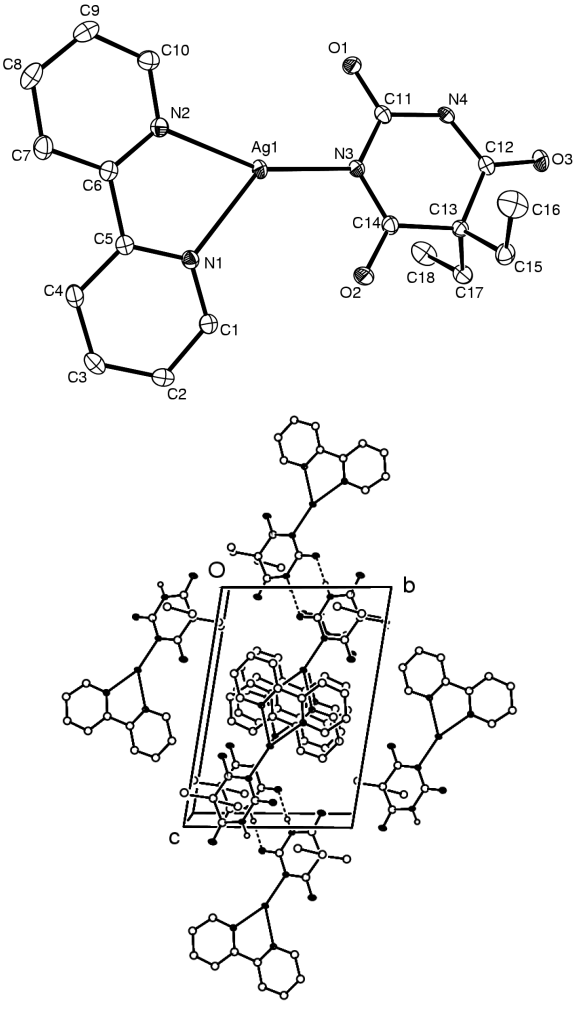

Fig. 1. Top: Molecular structure of **1**. C–H hydrogen atoms are omitted for clarity. Bottom: Packing diagram of **1**.

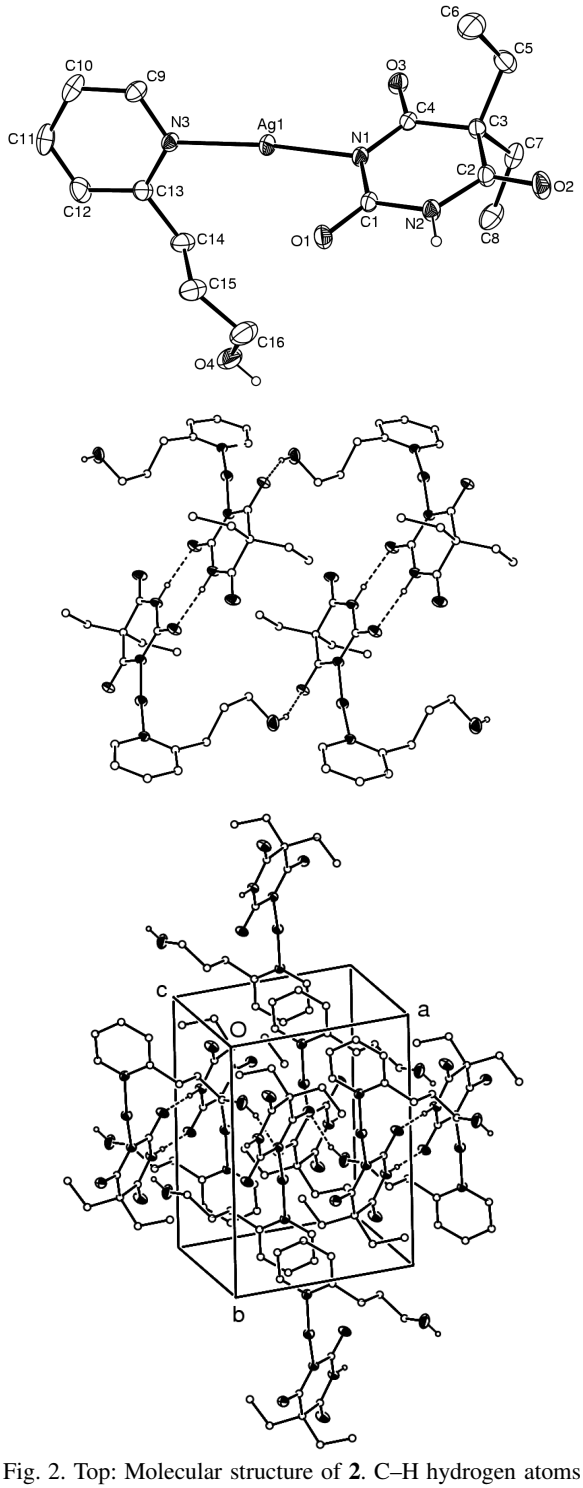

Fig. 2. Top: Molecular structure of **2**. C–H hydrogen atoms are omitted for clarity. Middle: View of hydrogen-bonded supramolecular assembly of **2**. Hydrogen bonds are indicated by dashed lines. Bottom: Packing diagram of **2**.

Both complexes crystallize in the triclinic system in space group $P\bar{1}$ with two formula units in the unit cell. The silver(I) ion in **1** is coordinated by a bpy ligand and a barb ligand, forming a significantly distorted T-shaped AgN_3 coordination with one N–Ag–N angle at 157.99(5)°. The bpy ligand chelates, forming a five-membered ring, while barb is N-coordinated. The bite angle of the bpy ligand is 71.54(4)° and significantly contributes to the distortion of the coordination geometry around the silver(I) ion.

The silver(I) ion in **2** is coordinated by a pypr ligand and a barb ligand, forming a slightly distorted linear AgN_2 motif with an N–Ag–N angle of 168.02(5)°. In contrast to the bidentate *N*- and *O*-donor ligand behavior in $[Co(pypr)_2(sac)_2]$ [9] and $[Cu(pypr)_2(sac)_2]$ [10], the pypr ligand acts as a monodentate ligand as in $[Ag_4(sac)_4(pypr)_2]$ [11]. The $Ag–N_{barb}$ bond lengths in **1** and **2** are identical, but are much longer than those found in the reported silver(I)-barb complexes $Na_3[Ag_3(\mu\text{-barb})_6]$ and $\{[Ag_2(\mu\text{-barb})_2][Ag_2(\mu\text{-en})_2]\cdot 5H_2O\}_n$ [7]. However, they are significantly shorter than the corresponding distances reported for $[Ag(barb)(\mu\text{-bpe})]_n$ [7].

The pyrimidine rings of the barb ligands in **1** and **2** are essentially planar and the three carbonyl groups are not significantly displaced from the mean planes of the rings. The individual molecules of **1** are doubly linked by N–H···O hydrogen bonds into dimers which are further connected by aromatic π(bpy)···π(bpy) stacking interactions [$C_g\cdots C_g(-x,\ 1-y,\ 1-z)$ = 3.8315 Å], leading to a three-dimensional network as shown in Fig. 1. Additionally, the crystal structure of **1** exhibit a number of X–H···Cg interactions involving the bpy and barb rings.

The molecules of **2** are connected into dimers by N–H···O hydrogen bonds between the barb units of the adjacent molecules. The dimeric units are linked by strong O–H···O hydrogen bonds involving the hydroxyl hydrogen of the pypr ligands and the carbonyl group of the barb ions, forming a hydrogen bonded supramolecular assembly (see Fig. 2). The pypr rings are also involved in weak aromatic $\pi\cdots\pi$ stacking [$C_g\cdots C_g(1-x, 2-y, 1-z)$ = 3.9133 Å] and C–H···π(pypr) interactions [C–H···$C_g(1-x,\ 1-y,\ 1-z)$ = 2.64 Å] reinforcing the three-dimensional network.

Thermal behavior

The decomposition of the complexes was followed up to 800 °C in a static atmosphere of air. Each com-

Table 2. Antimicrobial activity of compounds evaluated at minimum inhibitory concentrations as listed (MIC = $\mu g\,mL^{-1}$).

Compound	*P. aeruginosa*	*E. coli*	*B. subtilis*	*S. aureus*	*C. albicans*	*C. parapsilosis*
Na(barb)	> 100	> 100	> 100	> 100	> 100	> 100
bpy	> 100	> 100	> 100	> 100	> 100	> 100
pypr	> 100	> 100	> 100	> 100	> 100	> 100
$AgNO_3$	1.5	1.5	1.5	2	8	6
1	15	25	25	27	32	45
2	> 100	> 100	> 100	> 100	> 100	> 100
Ampicillin	> 100	50	55	10	–	–
Nystatin	–	–	–	–	7	3

plex shows a two-step decomposition behavior. Complex **1** is thermally stable up to 167 °C, while **2** begins to decompose at 118 °C. In the first decomposition stage of **1**, the endothermic elimination of bpy takes place between 167 and 284 °C with a mass loss of 35.1 % (calcd. 34.9 %). In the following stage in the temperature range 326 – 404 °C, an exothermic decomposition occurs. The decomposition of **1** ends at 380 °C and the total experimental mass loss value of 76.2 % agrees well with the calculated value of 75.8 %, assuming that the remaining solid residue is Ag_2O.

Complex **2** loses its pypr ligand in the temperature range 118 – 241 °C. For this stage, the experimental mass loss of 31.3 % is consistent with the calculated value of 32 %. The residue decomposes between 241 – 404 °C. The total mass loss of 73.7 % (total calcd. 74.7 %) suggests the formation of Ag_2O as the final decomposition product.

Antimicrobial activities

The *in vitro* antimicrobial activities of the free ligands and their silver(I) complexes were tested against two Gram-positive bacteria, *B. subtilis* and *S. aureus*, two Gram-negative bacteria, *E. coli* and *P. aeruginosa*, and two fungi, *C. albicans* and *C. parapsilosis*. The results are presented in Table 2 as minimum inhibitor concentration (MIC) values.

The antimicrobial activity of $AgNO_3$ was superior to that of both complexes against all of the bacterial and the fungal strains studied. The free ligands and solvents showed no antimicrobial activity against either bacterial or fungal strains tested at a concentration of 100 μg/mL. Comparing with the reference inhibitor ampicillin, **1** had a higher activity on all the strains except *S. aureus*. While *P. aeruginosa* was resistant to 100 $\mu g\,mL^{-1}$ ampicillin, **1** inhibited the growth at 15 $\mu g\,mL^{-1}$. The complex was about two fold more effective on *E. coli* and *B. subtilis* than ampicillin. In comparison with ampicillin, *S. aureus* was more resistant to **1**. However, a 27 $\mu g\,mL^{-1}$ MIC value is significant for *S. aureus*. Nystatin had a significant inhibitory effect on the fungal strains *C. albicans* and *C. parapsilosis*, at concentrations of 7 $\mu g\,mL^{-1}$ and 3 $\mu g\,mL^{-1}$ respectively, but **1** exhibited proportionally higher MIC values. The growth of *C. albicans* was inhibited at 32 $\mu g\,mL^{-1}$ while *C. parapsilosis* still grew up to the concentration of 45 $\mu g\,mL^{-1}$. Although **1** has a considerable inhibitory effect on the growth of all the strains tested at < 100 $\mu g\,mL^{-1}$, **2** has no inhibitory effect on all the strains at a concentration of 100 $\mu g\,mL^{-1}$. This may be a consequence of the slow precipitation tendency of **2** in the growth medium.

It has been suggested that the type of the coordinating ligands around silver(I) and the ease of their replacement are two important factors leading to a wide range of antimicrobial activities [12 – 13]. The Ag–N bond lengths in **1** are somewhat longer than those in **2**. This may result in a higher ligand exchange ability of **1** as compared to **2**.

Experimental Section

Materials and measurements

All reagents were commercially available and used without further purification. Elemental analyses (C, H, N) were carried out on an Elementar Vario EL elemental analyzer. The FT-IR spectra were recorded from KBr pellets in the range 4000 – 400 cm^{-1} by using a Mattson 100 FTIR spectrophotometer. ^1H NMR spectra were recorded at r. t. (298 K) with a Bruker AC200 spectrometer. Thermal analysis curves (TG and DTA) were obtained using a Rigaku TG8110 thermal analyzer in a static air atmosphere at a heating rate of 10 °C min^{-1}.

Synthesis of the silver(I) complexes

Na(barb) (5,5-diethylbarbituric acid sodium salt; 0.41 g, 2 mmol) dissolved in water (10 mL) was added to a solution of $AgNO_3$ (0.34 g, 2 mmol) in water (10 mL) with stirring whereupon a white polycrystalline solid formed. Bpy (0.32 g, 2 mmol) was added to the suspension and addition of 10 mL of 2-propanol resulted in a clear solution, which was allowed to stand at r. t. Colorless crystals of **1** were obtained after 2 d. Yield 67 %. – $C_{18}H_{19}N_4O_3Ag$ (447.24): calcd. C 48.34, H 4.28, N 12.53; found C 48.55, H 4.12, N 12.74.

Complex **2** was synthesized in a similar way using pypr instead of bpy. Yield 84 %. – $C_{16}H_{22}N_3O_4Ag$ (428.24): calcd. C 44.87, H 5.18, N 9.81; found C 45.06, H 5.30, N 9.63.

Antimicrobial testing

Standard strains of Gram-negative *Escherichia coli* MC4100 and *Pseudomonas aeruginosa* ATCC27853, Gram-positive *Bacillus subtilis* and *Staphylococcus aureus* ATCC 43300, and two yeasts *Candida albicans* ATCC 10231 and *C. parapsilosis* ATCC 22019 were used to test for antimicrobial activities of the compounds.

For antimicrobial activity tests, the broth dilution method was used as described by Yilmaz *et al.* [7]. The concentration at which no growth was observed was taken as MIC value (μg/mL), and represents the mean of at least three determinations. Ampicillin (Applichem) was used as a reference inhibitor for bacterial strains, nystatin (BDH) for fungal strains. For comparison, $AgNO_3$ was tested for MIC values. All the ligands and the solvents used were also tested for antimicrobial activity.

X-Ray crystallography

Intensity data for complexes **1** and **2** were collected using a Stoe IPDS 2 diffractometer. The structures were solved and refined using SHELXS-97 and SHELXL-97 [14]. All non-hydrogen atoms were found in a difference Fourier map and refined anisotropically. All CH hydrogen atoms in **1** and **2** were included using a riding model. The details of data collection, refinement and crystallographic data are summarized in Table 3.

CCDC 658607 (**1**) and 658608 (**2**) contain the supplementary crystallographic data for this paper. These data can be obtained free of charge from The Cambridge Crystallographic Data Centre *via* www.ccdc.cam.ac.uk/data_request/cif.

Table 3. Crystallographic data for complexes **1** and **2**.

	1	**2**
Empirical formula	$C_{18}H_{19}AgN_4O_3$	$C_{16}H_{22}AgN_3O_4$
M_r	447.24	428.24
Crystal size, mm^3	0.58×0.34×0.09	0.58×0.40×0.24
T, K	100(2)	296(2)
Radiation, λ, Å	0.71073	0.71073
Crystal system	triclinic	triclinic
Space group	$P\bar{1}$	$P\bar{1}$
a, Å	7.1503(6)	7.8031(7)
b, Å	9.3226(8)	10.9638(10)
c, Å	13.3963(12)	12.0605(11)
α, deg	99.428(7)	110.221(7)
β, deg	90.007(8)	106.118(8)
γ, deg	93.701(7)	97.762(7)
V, Å^3	879.04(13)	899.08(16)
Z	2	2
D_c, g cm^{-3}	1.690	1.582
μ, mm^{-1}	1.173	1.145
$F(000)$, e	452	436
θ range, deg	2.49/26.00	2.17/26.00
Index range h, k, l	±8, ±11, ±16	±9, ±13, ±14
Reflections collected	12708	13953
Independent reflections	3454	3541
R_{int}	0.027	0.058
Absorption correction	integration	integration
Min. / max. transmission	0.62 / 0.91	0.56 / 0.81
Data / parameters	3454 / 236	3541 / 217
Goodness-of-fit on F^2	1.082	1.022
Final R indices [$I \geq 2\sigma(I)$]	0.016	0.021
$wR2$ (all data)	0.041	0.051
Largest diff. peak/hole, e Å^{-3}	0.39/−0.48	0.28/−0.37

[1] J. N. Delgado, W. A. Remers, *Wilson and Gisvold's Textbook of Organic Medicinal and Pharmaceutical Chemistry*, 9th ed., J. B. Lippincott Company, Philadelphia, **1991**.

[2] L. Levi, C. E. Hubley, *Anal. Chem.* **1956**, *28*, 1591 – 1605.

[3] M. R. Caira, G. V. Fazakerley, P. W. Linder, L. R. Nassimbeni, *Acta Crystallogr.* **1973**, *B29*, 2898 – 2904.

[4] L. R. Nassimbeni, A. Rodgers, *Acta Crystallogr.* **1974**, *B30*, 1953 – 1961.

[5] F. Yilmaz, V. T. Yilmaz, C. Kazak, *Z. Anorg. Allg. Chem.* **2005**, *631*, 1536 – 1540.

[6] F. Yilmaz, V. T. Yilmaz, E. Bicer, O. Büyükgüngör, *Z. Naturforsch.* **2006**, *61b*, 275 – 280.

[7] V. T. Yilmaz, F. Yilmaz, H. Karakaya, O. Büyükgüngör, *Polyhedron* **2006**, *25*, 2829 – 2840.

[8] F. Yilmaz, V. T. Yilmaz, E. Bicer, O. Büyükgüngör, *J. Coord. Chem.* **2007**, *60*, 777 – 784.

[9] S. Hamamci, V. T. Yilmaz, W. T. A. Harrison, *J. Coord. Chem.* **2003**, *56*, 1033 – 1039.

[10] V. T. Yilmaz, S. Hamamci, O. Andac, C. Thone, W. T. A. Harrison, *Trans. Met. Chem.* **2003**, *28*, 676 – 681.

[11] V. T. Yilmaz, S. Hamamci, W. T. A. Harrison, C. Thone, *Polyhedron* **2005**, *24*, 693 – 699.

[12] K. Nomiya, K. Tsuda, T. Sudoh, M. Oda, *J. Inorg. Biochem.* **1997**, *68*, 39 – 44.

[13] K. Nomiya, R. Noguchi, M. Oda, *Inorg. Chim. Acta* **2000**, *298*, 24 – 32.

[14] G. M. Sheldrick, SHELXS/L-97, Programs for Crystal Structure Determination, University of Göttingen, Göttingen (Germany) **1997**.